The Astrophysical Journal, 860:22 (8pp), 2018 June 10 https://doi.org/10.3847/1538-4357/aabf85

The Redshift Completeness of Local Galaxy Catalogs

S. R. Kulkarni[1], D. A. Perley[2], and A. A. Miller[3,4]
[1] Division of Physics, Mathematics, and Astronomy, California Institute of Technology, Pasadena, CA 91125, USA; srk@astro.caltech.edu
[2] Astrophysics Research Institute, Liverpool John Moores University, IC2 Liverpool Science Park, Liverpool, L3 5RF, UK
[3] Center for Interdisciplinary Exploration and Research in Astrophysics (CIERA) and Department of Physics and Astronomy, Northwestern University, 2145 Sheridan Road, Evanston, IL 60208, USA
[4] The Adler Planetarium, Chicago, IL 60605, USA
Received 2018 April 11; revised 2018 April 17; accepted 2018 April 17; published 2018 June 7

Abstract

There is considerable interest in understanding the demographics of galaxies within the local universe (defined, for our purposes, as the volume within a radius of 200 Mpc or $z \leqslant 0.05$). In this pilot paper, using supernovae (SNe) as signposts to galaxies, we investigate the redshift completeness of catalogs of nearby galaxies. In particular, type Ia SNe are bright and are good tracers of the bulk of the galaxy population, as they arise in both old and young stellar populations. Our input sample consists of SNe with redshift $\leqslant$0.05, discovered by the flux-limited ASAS-SN survey. We define the redshift completeness fraction (RCF) as the number of SN host galaxies with known redshift prior to SN discovery, determined, in this case, via the NASA Extragalactic Database, divided by the total number of newly discovered SNe. Using SNe Ia, we find RCF $= 78\pm^{6}_{7}\%$ (90% confidence interval) for $z < 0.03$. We examine the distribution of host galaxies with and without cataloged redshifts as a function of absolute magnitude and redshift, and, unsurprisingly, find that higher-z and fainter hosts are less likely to have a known redshift prior to the detection of the SN. However, surprisingly, some L_* galaxies are also missing. We conclude with thoughts on the future improvement of RCF measurements that will be made possible from large SN samples resulting from ongoing and especially upcoming time-domain surveys.

Key words: galaxies: distances and redshifts – galaxies: statistics – supernovae: general

1. Transients in the Local Universe

Transients in the local universe provide unique insights into at least three pressing issues in modern astronomy. First, nearby events can be studied in great detail, even if their luminosities are relatively low—enabling insights into their physics. A classic example is the detection of SN 1987A in the Large Magellanic Cloud, which enabled the unambiguous localization of extragalactic neutrinos (e.g., McCray 1993). Second, nearby events can be studied demographically to high completeness. This is important both for obtaining a full understanding of how stars end their lives and for understanding the role their explosions play in their environments. For example, supernovae (SNe), the most commonly observed extragalactic transients, inject energy, momentum, and heavy elements into their surroundings. Relating star formation rate and chemical abundance to SN rates is a fundamental exercise in modern astronomy. Nearby (volume limited) SN surveys are needed to provide the latter.

Third, over the last decade or so, exotic explosive sources have been identified—Ultra High Energy Cosmic Rays (UHECR), ultra-high energy neutrinos, and Gravitational Wave (GW) sources. The horizon for detecting these sources is limited by either physical phenomena (the Greisen–Zatespin–Kuzmin effect for UHECRs), or set by the sensitivity of GW telescopes.[5] The latter consideration leads us to a distance limit of ∼200 Mpc ($z \lesssim 0.05$). As shown by the rich returns from electromagnetic studies of the neutron star coalescence event, GW170817 (e.g., Abbott et al. 2017a, 2017b), the study of transients in the local universe is not only of wide importance but is also timely.

The primary motivation for this paper is the last point discussed above, namely the study of electromagnetic counterparts to GW sources. For the next few years, the typical localization of GW sources will be no better than ∼50 deg^2. Naturally, pursuit of such large angle localizations will entail a deluge of false positives (e.g., Kasliwal et al. 2016; Smartt et al. 2016). As demonstrated by the steps that led to the discovery of the optical counterpart of GW170817, a cost-effective approach to both minimizing the background fog of false positives and maximizing early identification is to use on-sky coincidences with catalogs of nearby galaxies (e.g., Gehrels et al. 2016).

Additionally, we note that catalogs of nearby galaxies have other uses. For instance, there is considerable interest in studying the youngest SNe. SNe take time to brighten to peak luminosity and are very faint in the first hours to days after the initial explosion, so the appearance of a new source with an inferred luminosity much lower than a classical SN at peak is cause for vigorous pursuit. But determining this luminosity requires knowledge of the redshift, which will be known in advance only if the transient coincides with a galaxy with a cataloged redshift.

As a result of deep wide-field imaging surveys, such as PanSTARRS-1 (PS1) and the Sloan Digital Sky Survey (SDSS), all galaxies, particularly in the Northern sky, to ∼23 mag, are "cataloged" (in the sense that multi-band photometric measurements exist, and the galaxies are assigned a nominal name).[6] However, what matters for the purpose of this paper is a *reliable* galaxy redshift measurement, *prior* to any transient follow up (such as during a search for EM counterparts). The fraction of nearby galaxies of a certain type

[5] In this paper, we restrict the discussion of GW sources to those involving neutron stars, as electromagnetic (EM) counterparts are only expected for such events.

[6] Separating stars from galaxies in these photometric catalogs presents a significant challenge, however.

(for example, candidate hosts of LIGO GW sources) with a redshift that is recorded in published catalogs can be defined as the redshift "completeness."[7]

In this paper, we explore the use of SNe to assess the completeness of nearby galaxy catalogs. SNe are very luminous, relatively common (in a cosmological sense), and are found routinely in surveys that now cover the entire sky every few days (and therefore the entire local volume out to some distance limit, subject to the limitation of extinction from the Galactic plane). Thus, they provide an effective way of randomly sampling galaxies that is not strongly dependent on the observational properties of those galaxies (in particular, on galaxy luminosity). Recently, Holoien et al. (2017a) remarked that 24% of nearby bright SNe were discovered in cataloged host galaxies without secure redshifts, suggesting that redshift incompleteness may be significant even today. As a next step, we refine their estimate by formally restricting their sample to a limited volume and examine in detail those SNe that occur in galaxies whose redshifts have been "missed" by spectroscopic surveys.

2. Catalogs of Nearby Galaxies

The construction of redshift catalogs for meaningful numbers of nearby galaxies can only be accomplished via large-scale spectroscopic surveys (e.g., Blanton & Moustakas 2009). However, given the more than eight magnitude spread in galaxy luminosities (Blanton & Moustakas 2009), large numbers of even very nearby galaxies are likely to be quite faint, so these catalog(s) will necessarily be incomplete. Despite this challenge, astronomers have assembled a number of all-sky galaxy catalogs: the 11 Mpc *Updated Nearby Galaxy Catalog* (Karachentsev et al. 2013), *The Extragalactic Distance Database* (Tully et al. 2009), and *Hyperleda* (Paturel et al. 2003). These catalogs are linked to the NASA/IPAC Extragalactic Database (NED).[8] Figure 1 of Gehrels et al. 2016 provides a graphical illustration of the bias of inputs to spectroscopic surveys.

How complete are these catalogs? One approach is to extrapolate the findings of higher-z surveys (which scrutinize small areas of the sky down to extremely deep limits) down to $z \approx 0$. However, as shown by deviations of galaxy recession velocities from the Hubble flow (Jha et al. 2007) and via direct galaxy catalogs, the local universe is lumpy (10% fluctuations or more) on length scales as large as 200 Mpc.[9] Extrapolating a local catalog believed to be highly complete (e.g., *Nearby Galaxy Catalog*, which is complete to $M_B < -15$ mag within 11 Mpc outside the Galactic plane) from the bottom up is even more problematic given strong fluctuations on these distance scales (e.g., not a single galaxy cluster lies within 11 Mpc).

3. Assessing Catalog Completeness with SNe

Here, we explore the use of SNe to evaluate the completeness of catalog(s) of the nearby universe. Type Ia SNe are well suited for this task. These SNe are luminous (only $\sim$1 mag fainter than a local L_* galaxy in the V band) and thus easily identified. The luminosity function is narrow: in the B band, the luminosity function can be fit with a Gaussian with a mean value of -19.4 mag and an rms of 0.14–0.23 mag (Yasuda & Fukugita 2010). Next, SNe Ia arise from both old and young populations (Scannapieco & Bildsten 2005; Sullivan et al. 2006). Thus, they sample all types of galaxies and can be used to study galaxy demographics without missing significant subpopulations.

In contrast, core-collapse SNe (CC SNe) arise only in star-forming galaxies and exhibit a wide luminosity function, with absolute magnitude (SDSS r band) ranging from -18 to -12 (Taylor et al. 2014). Clearly, additional care is necessary in using CC SNe to measure the RCF.

Our proposal to assess the completeness of nearby galaxies catalogs is simple: (1) Following the detection of an SN, measure the redshift of the host galaxy, $z_{\rm host}$. (2) Retain those events with $z_{\rm host} \leqslant z_*$, where z_* is the redshift to which the completeness is being measured ("tries"). (3) Check the galaxy catalog(s) to see if the SN host galaxy has a reliable redshift entry. If present and if $z_{\rm host}$ is equal to $z_{\rm SN}$ to within approximately 0.001, then it is a "hit." The redshift completeness factor (RCF) of the galaxy catalog is given by the ratio of "hits" to "tries."

We emphasize that our definition of the RCF is explicitly tied to SNe and is not the fraction of galaxies with known redshifts *by number*. The majority of galaxies within any volume are very small galaxies, which are also the most difficult to detect (indeed, new satellites of the Milky Way are still being uncovered). Previous studies (Scannapieco & Bildsten 2005; Sullivan et al. 2006) have found that the Ia propensity (the rate of Ia production within a galaxy), $\mathcal{P}$, is well represented by a linear combination of the stellar mass of the galaxy ($\mathcal{M}$) and the star formation rate ($\mathcal{S}$). Thus, the RCF (as defined here) approximately measures the completeness weighted by $\mathcal{P}$. Other definitions could be used; for example, had we employed CC SNe instead of SNe Ia, the resulting RCF would measure the completeness weighted by $\mathcal{S}$ alone.

SN-based estimates of the RCF will depend on the completeness of the parent SN survey(s). An SN survey that is not complete to the limit of the search volume will find a larger fraction of low-luminosity events at smaller distances whereas more luminous events can be found to larger distances (with concomitant larger volume). Thus, poor control of completeness in an SN survey will bias the sample toward galaxies that host more luminous events. In the case of Ia SNe, a correlation between the luminosity of the SN and the properties of its host does exist (Sullivan et al. 2010), although it is relatively weak. A larger concern is whether the properties of the host directly affect completeness or not, e.g., if SNe are systematically missed in regions of high galaxy surface brightness or if the appearance of the host galaxy is a consideration in decisions about spectroscopic classification.

We emphasize that the SN rate per galaxy is far too low to provide a practical means of actually discovering new galaxies in significant numbers. Instead, the approach advocated here provides a check on the completeness of *existing* catalogs, independent of the traditional luminosity function approach.

4. Primary Data

To assess the RCF, we use NED as our input host galaxy catalog and the first two SNe catalogs (hereafter, A1, A2) published by the All-sky Automated Survey for SN (ASAS-SN) project (Holoien et al. 2017a, 2017b; hereafter, H1 & H2, respectively). ASAS-SN is well suited for our purposes. It is a

[7] We will more precisely state our operational definition of "completeness" in Section 3.

[8] https://ned.ipac.caltech.edu/

[9] This is not at all surprising given the 150 Mpc Baryon Acoustic Oscillations (BAO) length scale.

Table 1
SN Demographics from the Two ASAS-SN Surveys

Catalog	Type[a]	n(SN)	n(NED$_z$)
A1	Ia	66	51
A1	CC	25	22
A2	Ia	141	101
A2	CC	39	27

Note. n(SN) is the number of SNe in each category. n(NED$_z$) is the number of host galaxies with a redshift entry in NED (and obtained prior to the SN discovery).
[a] The type Ia encompasses normal Ia and all subtypes such as 91T, 91bg, CSM and 00cx. All non-Ia SN are called as core collapse (II, IIn, Ibc).

flux-limited survey, $V_{\rm peak} \leqslant 17$ mag, that covers the entire sky and is not targeted to specific galaxies. Additionally, because of its shallow flux limit, ASAS-SN candidates are bright enough for worldwide follow up using small telescopes. As a result, the classification (SN type and $z_{\rm host}$) is essentially complete. In contrast, amateur discoveries (as well as professional surveys such as LOSS, the Lick Observatory SN Survey; Li et al. 2000) target well-resolved and bright galaxies and are therefore biased. Other, recent untargeted surveys (e.g., ATLAS, iPTF, *Gaia*) are not likely to be strongly biased in terms of discovery, but the degree of bias in terms of selecting candidates to follow up (and classify as SNe) is not well-quantified.

Table 1 provides a top-level summary of the two ASAS-SN surveys. Catalog A1 lists 91 SNe discovered during the period 2013–2014 (H1). Catalog A2 lists 180 SNe found in the calendar year 2015. In A2 11, SNe are marginally fainter than 17 mag (H2). The catalogs also include host galaxy data: name, redshift, SDSS, *GALEX* , 2MASS, and *WISE* photometry.

H1 and H2 do not specifically identify host galaxies that lack a cataloged redshift prior to the discovery of the SN. To remedy this situation, we wrote a program to query NED and obtained the redshifts of the putative host galaxies. We refer to the sample of galaxies with a redshift entry in NED as the "NED$_z$" sample and those which lacked an entry as the "!NED$_z$" sample.

Nine entries (ASAS-SN-15de, 15ji, 15jm, 15lh, 15nh, 15og, 15ts, 15 ua, 14ms) have $z_{\rm host} > z_* = 0.05$. These were deleted from further consideration. Next, we inspected the difference between the SN redshift, $z_{\rm SN}$, and the purported host redshift given in NED, $z_{\rm host}$. Bearing in mind the lower precision of the SN redshift, we made an allowance and inspected events with $|z_{\rm host} - z_{\rm SN}| > 10^{-3}$. The rationale for this choice is that the redshift of the host is usually the systemic velocity of the galaxy (a fiber of the spectrograph encompasses the central region of the galaxy) whereas the SN will have additional velocity arising from the rotation curve. Three events stood out: ASASSN-15jo has $z_{\rm host} = 0.014$ (Abell S0753), but $z_{\rm SN} = 0.011$; ASASSN-13an has $z_{\rm host} = 0.02431$ (2MASX J13453653−0719350), but $z_{\rm SN} = 0.0216$; and ASASSN-15ic has $z_{\rm host} = 0.0637$ (2MASX J06145320−4247357), $z_{\rm SN} = 0.025$. We retain the first two events and delete the last one from further consideration. The final sample for the analysis reported below consists of 261 SNe.

5. Analysis

The redshift distribution of ASAS-SN events is displayed in Figure 1. SNe Ia peak at $z \approx 0.025$ whereas CC events peak at lower redshift and exhibit long tails (as expected, given their lower average luminosities and broad luminosity function). The "completeness" of the SN sample itself is not the primary topic of this paper.[10] What is central to this paper is that the SN sample not be biased by host galaxies. Thus, we will proceed with the analysis of the sample we have in hand. The RCF, assuming NED as the input host galaxy catalog, for $z_{\rm host} \lesssim 0.03$ is 80% ± 5% (90% confidence interval; see Table 2). The precision of these estimates is limited by small-number binomial statistics. The RCF as traced by SNe Ia, furthermore, is somewhat lower ($78\pm^{6}_{7}$%) than the RCF traced by CC SNe ($87\pm^{5}_{9}$%), suggesting that galaxy catalogs are more complete for star-forming hosts. The precision of these estimates is limited by small-number binomial statistics. For our full sample ($z_{\rm host} \lesssim 0.05$), there are 64 !NED$_z$ galaxies, which corresponds to RCF = $75\pm^{5}_{4}$%.

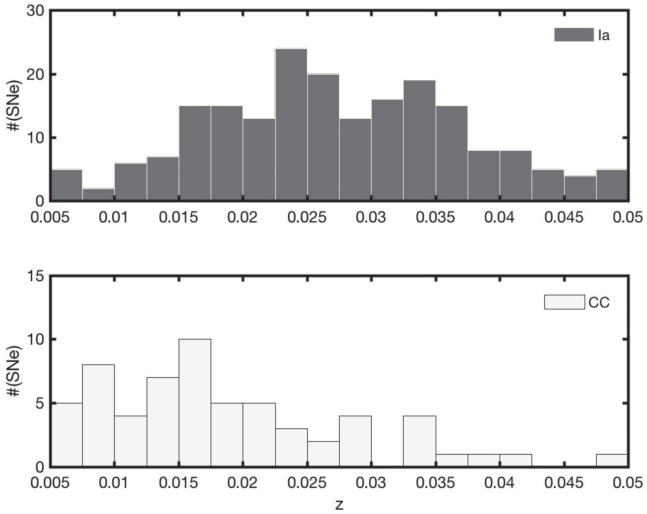

Figure 1. Histogram of $z \leqslant 0.05$ SNe of type Ia (top) and core-collapse (bottom) from the A1 and A2 catalogs.

Table 2
Redshift Completeness Factor of ASAS-SN SNe ($z < 0.03$)

SN	n(SN)[a]	n(NED$_z$)[b]	n(!NED$_z$)[c]	RCF[d]
All	173	139	34	0.75–0.85
Ia	120	93	27	0.71–0.83
CC	53	46	7	0.78–0.93

Notes.
[a] The total number of SNe.
[b] The number of SNe with a putative host galaxy with redshift listed in NED, prior to SN discovery.
[c] The number of SNe with a putative host galaxy but whose redshift is not listed in NED.
[d] The Redshift Completeness Factor (RCF; see Section 3) range covers a confidence range of 5%–95% and is obtained by assuming a flat Bayesian prior.

6. Analysis of Host Galaxy Luminosities

The virtue of the SN RCF is that it is a well-defined and simple metric, with no free parameters other than the distance (volume) limit employed. However, within this volume, we generally expect the completeness to be higher for luminous galaxies (with high stellar mass $\mathcal{M}$, or high star formation rate $\mathcal{S}$) than less luminous ones. Knowing these parameters for the

[10] Understanding the completeness of an SN survey is a major project in itself!

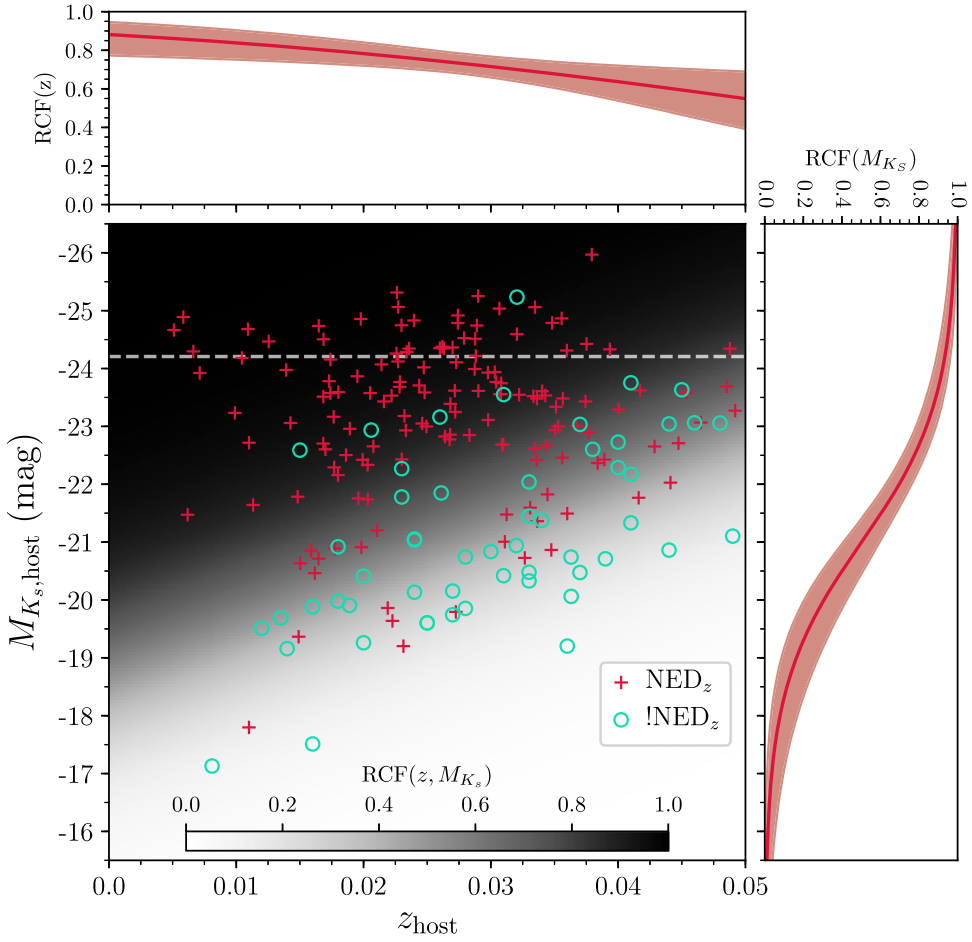

Figure 2. Absolute K_s-band magnitude, $M_{K_s,\mathrm{host}}$, vs. redshift, z_{host}, for the host galaxies of SNe Ia in A1 and A2. Galaxies with redshift entries in NED are shown as red pluses, while those lacking redshifts (!NED$_z$) are shown as teal circles. The horizontal dashed line shows $M^*_{K_s}$. The shaded background shows the probability of a host galaxy having a cataloged redshift given its redshift and M_{K_s} (RCF(z, M_{K_s}); see Appendix A for details). The top and right plots show the probability of a host galaxy having a cataloged redshift given *only* its redshift, RCF(z), *or* M_{K_s}, RCF(M_{K_s}), respectively. In these two plots, the solid lines show the median value of the RCF, while the shaded area corresponds to the 90% bound on the RCF.

galaxies within our sample, we can subdivide our targets by $\mathcal{M}$ or $\mathcal{S}$ to answer interesting questions such as, "How complete is our understanding of $\mathcal{M}$ / $\mathcal{S}$ within the local volume"? For this purpose, we use the 2MASS K_s-band as a proxy for $\mathcal{M}$ and the *GALEX* NUV band for $\mathcal{S}$ and examine the completeness as a function of these two parameters.

H1 & H2 took K_s-band magnitudes from 2MASS when available; otherwise, a K_s-band mag was estimated from *WISE* $W1$ when detected in that band (offset by a typical $K_s - \mathrm{W}_1 = -0.64$ mag), or (in the absence of both 2MASS and *WISE*) a limit of $K_s > 15.6$ mag was set. We employ the same approach using their magnitude catalogs, except that for the last group (three galaxies in catalog A1 and five in catalog A2), we simply set $K_s = 15.6$ mag.[11]

In A1, there are 77 SNe with NUV data, 5 with only SDSS u' data and 9 with neither NUV nor u' data. In A2, the corresponding numbers are 138, 17, and 24, respectively. We took the sample of SNe with both NUV and u' data, applied the Galactic extinction correction, and found the median of NUV$-u' \approx 1$ mag. We use the NUV data when available and u' with the aforementioned offset applied otherwise. We call this hybrid magnitude the "UV" mag. The 32 SNe with neither NUV nor u' data are not included in the analysis.

For the discussion below, we note that the relevant Schechter characteristic luminosity parameters are $M^*_{K_s} = -24.2 \pm 0.03$ (Cole et al. 2001) and $M^*_{\mathrm{NUV}} = -18.23 \pm 0.11$ (Wyder et al. 2005). Below, we examine the missing galaxies with luminosity $L > L_*$ in both the K_s and "UV" bands. We then isolate the sample to just Type Ia SNe to investigate missing galaxies with $L < L_*$.

6.1. K_s-band

The absolute K_s-band magnitude, $M_{K_s,\mathrm{host}}$, and redshift, z_{host}, of each SN Ia host galaxy in our sample is displayed in Figure 2.[12] We calculate the distance modulus to each host using `CosmoCalc` (Wright 2006) and z_{host}, where we have assumed $\Omega_\Lambda = 0.714$, $H_0 = 69.6$ km s^{-1} Mpc^{-1}, and $\Omega_m = 0.286$. The joint distribution for a host galaxy to have a previously cataloged redshift given its redshift and M_{K_s}, RCF(z, M_{K_s}), along with the one-dimensional probabilities, RCF(z) and RCF(M_{K_s}), are also shown in Figure 2. Details for

[11] We note that catalog magnitudes may sometimes significantly underestimate the total flux of extended sources due to the presence of significant flux outside the automatically defined aperture (T. H. Jarrett et al. 2018, in preparation). We neglect this effect in our pilot study but note that any detailed characterization of the host population probed by nearby SNe would require careful attention to this issue.

[12] CC SNe are considered in Appendix B.

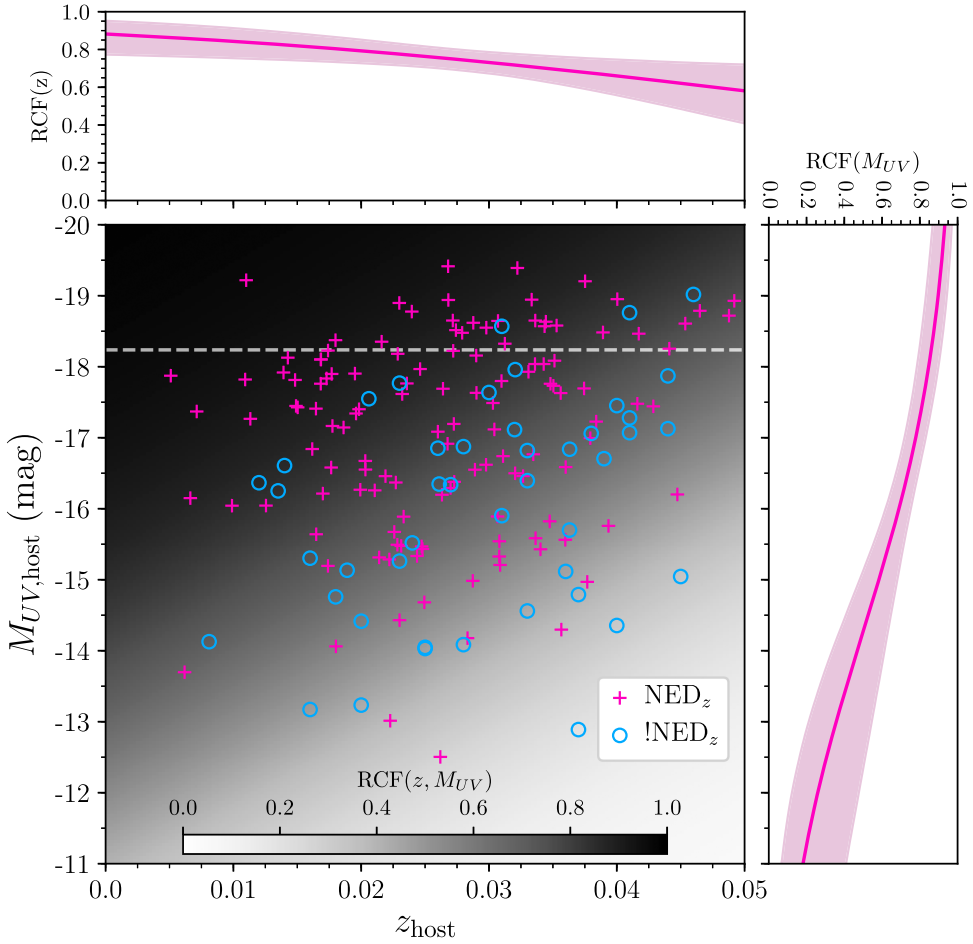

Figure 3. Absolute "UV"-band magnitude, $M_{\mathrm{UV,\ host}}$, vs. redshift, z_{host}, for the host galaxies of SNe Ia in A1 and A2. Galaxies with redshift entries in NED are shown as magenta pluses, while those lacking redshifts (!NED$_z$) are shown as blue circles. The horizontal dashed line shows M^*_{UV}. The shaded background shows the probability of a host galaxy having a cataloged redshift given its redshift and M_{UV} (RCF(z, M_{UV}); see Appendix A for details). The top and right plots show the probability of a host galaxy having a cataloged redshift given *only* its redshift, RCF(z), *or* M_{UV}, RCF(M_{UV}), respectively. In these two plots, the solid lines show the median value of the RCF, while the shaded area corresponds to the 90% bound on the RCF.

these calculations are presented in Appendix A. Figure 2 confirms the intuitive results that the RCF is lower for higher redshift and intrinsically fainter galaxies.

In total, there are 42 host galaxies brighter than $M^*_{K_s}$, and 2 of these did not have redshift entries in NED prior to SN discovery. The first is the host of ASASSN-15ed, MCG +09-27-087/SDSS J164825.26+505935.5, a bright, large (40″) spiral galaxy. There is no SDSS spectroscopic redshift but the SDSS photoz estimate is 0.031 ± 0.01. The host galaxy has a 10.2 ± 1.1 mJy counterpart in NVSS. The second is the host of ASASSN-15ub, CGCG 314-006. Nominally, there is no host redshift in NED. However, a direct inspection of SDSS shows a pair of strongly interacting galaxies with a spectroscopic redshift of 0.032 (photoz of 0.027 ± 0.0076), which can be compared to $z_{\mathrm{SN}} = 0.032$.

We restrict the analysis of sub-luminous galaxies to SNe Ia. In the K_s band, there are 163 host galaxies with $L < L_*$. Of these, 110 are listed in NED. Thus, as traced by SNe Ia, the RCF = [67%–73%] (5%–95% confidence range).

6.2. NUV/u' Band

As was the case for K_s band, the median !NED$_z$ host galaxy is ∼2 mag fainter than the median NED$_z$ host galaxy for the "UV" band (Figure 3). The redshift distribution of NED$_z$ and !NED$_z$ galaxies is nearly identical in K_s and "UV," with higher-z hosts more likely to not be included in NED. The peak of the !NED$_z$ sample "UV" luminosity is not as biased toward faint galaxies as it is in the K_s band. This conclusion bodes well for the PTF Census of the Local universe Hα survey, which is searching for nearby star-forming galaxies (Cook et al. 2017).

In the "UV" band, 46 galaxies are brighter than L_*, and 5 of those are !NED$_z$ galaxies. The host of ASASSN-15ed, MCG +09-27-087; SDSS J164825.26+505935.5, is discussed above. The ASASSN-15ln host, GALEXASC J225332.83+194232.9, is a 10″ spiral galaxy with no SDSS spectroscopic redshift but an SDSS photoz of 0.022 ± 0.0092. The host of ASASSN-15ho, 2MASXi J0909234-044327, lies outside the SDSS footprint. The hosts of ASASSN-15sh and ASASSN-15um, 2MASX J19320827-6226340 and 2MASX J05395948-8022191, respectively, lie in poorly studied regions of the sky.

Again, we restrict the analysis of missing sub-luminous galaxies to SNe Ia hosts. There are 140 galaxies with "UV" luminosity less than the corresponding L_* value. Of these, 98 have redshift entries in NED. Thus, as traced by SNe Ia, the RCF = [63%–76%].

7. Increasing the Precision and Accuracy of RCF

The ASAS-SN bright SN sample is attractive for measuring the RCF due to its host-unbiased approach and the essentially complete spectroscopic classification of all candidates that results from its shallow magnitude limit. However, owing to the small sample size, the RCF estimates are limited by binomial errors. We undertook a similar analysis for a larger sample: SNe candidates reported at the Transient Name Server (TNS)[13] portal, during the period between 2016 January and 2017 June. The sample spans a larger peak magnitude range relative to ASAS-SN, extending as faint as 20 mag. Nonetheless, it appears that follow up was obtained for most of the reported candidate SNe. The resulting sample size is 529 nearby ($z \leqslant 0.05$) SNe. We find that the RCF for this sample is similar to that derived for the ASAS-SN sample (B. Cassese & S. R. Kulkarni 2018, in preparation).

The field of optical time-domain astronomy is in a boom period, and much larger samples of nearby SNe can be expected given the Asteroid Terrestrial-impact Last Alert (ATLAS; Tonry 2011), PanSTARRS-1 (Wainscoat et al. 2016), Zwicky Transient Facility (ZTF; Dekany et al. 2016; Bellm & Kulkarni 2017), and upgraded ASAS-SN surveys. The limiting V-band magnitudes for these surveys range from 17 to 21 mag. Below, we consider the gains resulting from large SN samples.

To make this discussion more concrete, we consider a specific example, the "Celestial Cinematography" survey of ZTF (Bellm & Kulkarni 2017). This survey aims to systematically cover a large fraction of the night sky ($\gtrsim$12,000 deg^2) every three nights, in the g and R bands. The median 5σ detection limit for a fixed 30 s exposure time is 20.5 mag. The annual volumetric rates of $z \approx 0$ Type Ia and CC SNe are $\mathcal{R}_{\rm Ia} \approx 3 \times 10^4\,{\rm Gpc^{-3}\,yr^{-1}}$ and $\mathcal{R}_{\rm CC} \approx 7 \times 10^4\,{\rm Gpc^{-3}\,yr^{-1}}$, respectively (Li et al. 2011). Based on a simulator built for ZTF, the expected annual yield for the above survey is [230, 460, 892, 1750] for peak magnitude of [17.5, 18, 18.5, 19] mag, respectively (U. Feindt 2018, personal communication).

Going forward, we will assume a "Bright Transient Survey" (BTS) whose goal is to classify all extragalactic transients with peak magnitudes brighter than 18.5 mag. A one-year survey would result in a sample of nearly 1000 SNe Ia. With this sample, a regional RCF can be evaluated (e.g., high and intermediate Galactic latitude regions). Next, the large and unbiased sample would allow for a number of other applications, including self-consistent checks of the dependence of the SN Ia rate on host type, which is frequently formulated as $\mathcal{P} \propto a\mathcal{M} + b\mathcal{S}$ (Scannapieco & Bildsten 2005); here, a and b are constants. Deviations will provide us with insight into a better formulation of the relationship between $\mathcal{P}$ and $\mathcal{M}$ and $\mathcal{S}$.

Such a large survey would, in its own right, be interesting. For example, determining volumetric SN rates from untargeted, wide-field surveys requires the identification of all galaxies within a specified distance. The BTS measurement of the RCF will provide the correction factors needed to account for missing galaxies when calculating the volumetric rates. For example, the relative rate of SN 2002cx-like (SNe Iax) to normal SNe Ia is wildly uncertain (≈5%–30%; e.g., Li et al. 2011; Foley et al. 2013; Miller et al. 2017), and the large sample from the BTS will substantially improve these estimates. Furthermore, such a large, low-redshift sample would be very valuable for Ia SN cosmography (e.g., Goliath et al. 2001; Scolnic et al. 2017).

Next, we address CC SNe. As noted in Section 3, CC SNe exhibit a wide range in peak magnitude: M_r ranging from −12 to about −18 mag (Taylor et al. 2014). The BTS is well suited to determining the demographics of CC SNe. A survey complete to a flux limit $V \approx 18$ mag will detect SNe peaking at $M_V = -12$, −15, and −18 mag to radii of ∼10, 40, and 160 Mpc, respectively. The total number of CC SN detections will sharply depend on the luminosity function. For instance, Taylor et al. (2014) suggest that the fraction of CC SNe fainter than −15 mag at peak is at least 24% but can be as high as 50%. In any case, BTS will allow us to measure the luminosity function of CC events, which is essential to determine the volumetric rate of CC SNe. In turn, the latter is a key element in our understanding of stars and the interstellar medium (Horiuchi et al. 2011). Finally, while CC SNe certainly track $\mathcal{S}$, it may be the case that "lesser" parameters, such as metallicity, change the mix of CC SNe subtypes (Arcavi et al. 2010; Galbany et al. 2016; Graur et al. 2017). Again large-sample SN surveys may well have sufficient diagnostic power to ferret out such connections.

It is increasingly evident that the primary limitation to SN surveys is limited by our ability to spectrally classify the SN candidates. This load can be made bearable by the use of two spectrographs: an ultra-low-resolution spectrometer tuned to classification and a standard low-resolution spectrometer to obtain the redshift and gross spectrum of the host galaxies. For the latter, we note that within a few years not merely highly but *supremely* multiplexed spectrographs (e.g., DESI,[14] PFS[15], and the planned AS4 project) will be commissioned. These facilities, at very little cost (small fractional allocation of fibers), can measure the redshifts of host galaxies of SNe on an industrial scale. The same highly multiplexed spectrographs will likely be pressed into surveys more ambitious than SDSS or 6dF, leading to more complete catalogs of galaxies in the nearby universe.

We thank the anonymous referee as well as A. Goobar, U. Feindt, C. Pankow, M. Kasliwal, P. Nugent, E. O. Ofek, E. S. Phinney, K. Taggart, and H. Vedantham for input and helpful discussions.

AAM is funded by the Large Synoptic Survey Telescope Corporation in support of the Data Science Fellowship Program.

Software: `emcee` (Foreman-Mackey et al. 2013), `corner` (Foreman-Mackey 2016), `matplotlib` (Hunter 2007; Droettboom et al. 2018), `scipy` (Jones et al. 2001), `pandas` (McKinney 2010), `CosmoCalc` (Wright 2006).

Appendix A
Conditional Probability of the RCF

We aim to characterize the RCF as a function of redshift, z, and host galaxy luminosity, where we use either $M_{K_s,\rm host}$ or $M_{\rm UV,host}$ as a proxy. To do so, we model the data X with the Bernoulli distribution

$$X \sim {\rm Bern}(p), \tag{1}$$

where p is parameterized with a logistic function with dependence on both redshift z and host galaxy luminosity

$$p(z, M, \theta) = \frac{1}{1 + \exp(az + bM - c)}, \tag{2}$$

[13] https://wis-tns.weizmann.ac.il/

[14] http://desi.lbl.gov

[15] http://pfs.ipmu.jp

with host-galaxy absolute magnitude M, and θ representing the model parameters a, b, and c, which need to be determined. The precise analytic dependence of p on z and M may not be logistic; however, the purpose of this exercise is to provide a general sense for how the RCF relies on z and M. The logistic function is ideal for this general purpose.

From here, it follows that the probability of a host galaxy having a previously cataloged redshift is

$$Pr(q) = \begin{cases} p(z, M, \theta), & \text{if } q = \text{NED}_z \\ 1 - p(z, M, \theta), & \text{if } q = \ \text{!NED}_z \end{cases} \quad (3)$$

and the likelihood of the observations given the data and model parameters is

$$Pr(q_k \mid z_k, M_K, \theta) = \prod_{k=1}^{K} p(z_k, M_k, \theta)^{q_k} \times (1 - p(z_k, M_k, \theta))^{1-q_k}, \quad (4)$$

where k represents the individual observations and $q_k = 1$ for NED_z galaxies and $q_k = 0$ for ! NED_z galaxies.

From Bayes' theorem, we can multiply the likelihood by a prior, $Pr(\theta)$, and use Markov Chain Monte Carlo (MCMC) techniques to sample from the posterior $Pr(\theta \mid q_k, z_k, M_K)$ in order to constrain the model parameters θ. We use the `emcee` package (Foreman-Mackey et al. 2013) to implement our MCMC sampling of the posterior. For a and b, we adopt flat priors bounded between 0 and 10^6. For c, we adopt a flat prior between -100 and 100. Following the MCMC sampling, we find that there is a strong covariance between b and c, while a is relatively independent of b and c. The shading in Figures 2 and 3 shows $p(z, M, \theta)$ for the maximum a posteriori sample from the MCMC sampling.

We additionally wish to constrain the behavior of the RCF as a function of either the host redshift, z, or host galaxy luminosity. We do this separately from the analysis above, while using the same MCMC procedure with p in Equations (3) and (4) replaced by

$$p(z, \theta) = \frac{1}{1 + \exp(az - c)}, \quad (5)$$

for redshift, and

$$p(M, \theta) = \frac{1}{1 + \exp(bM - c)}, \quad (6)$$

for host galaxy luminosity (where, again, we use absolute magnitude M as a proxy). The results of this procedure are shown in the side panels of Figures 2 and 3. In these panels, the solid lines show the median value of $p(z)$, RCF(z) in the Figures, and $p(M)$, RCF(M) in the Figures, from all the posterior samples, while the shaded region shows the 90% credible regions for $p(z)$ and $p(M)$ from the posterior samples. We close by noting that the current data set provides weak constraints on a in Equation (5), but these constraints will be greatly improved by the BTS, which will include a significantly larger sample and extend to higher redshifts.

Appendix B
RCF as Traced by CC SNe

The CC SNe samples in A1 and A2 are insufficient to meaningfully constrain the RCF as a function of redshift or host galaxy absolute magnitude. Furthermore, CC SNe only trace star formation, meaning they do not probe passive galaxies, so we have excluded them from the analysis in the main text. Nevertheless, for completeness, we show the host galaxies for CC SNe in Figure 4.

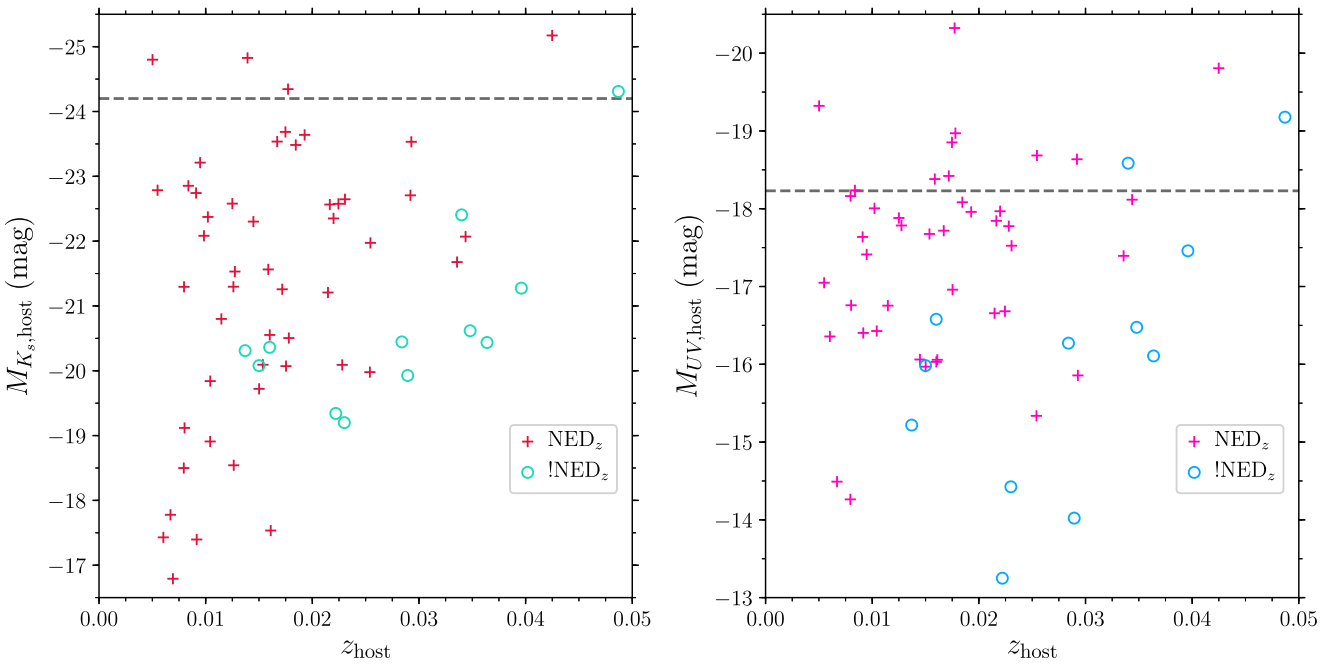

Figure 4. Left panel: absolute K_s-band magnitude, $M_{K_s,\text{host}}$, vs. redshift, z_{host}, for the host galaxies of CC SNe in A1 and A2. Galaxies with redshift entries in NED are shown as red pluses, while those lacking redshifts (!NED$_z$) are shown as teal circles. The horizontal dashed line shows $M^*_{K_s}$. Right panel: absolute "UV"-band magnitude, $M_{\text{UV, host}}$, vs. redshift, z_{host}, for the host galaxies of CC SNe in A1 and A2. Galaxies with redshift entries in NED are shown as magenta pluses, while those lacking redshifts (!NED$_z$) are shown as blue circles. The horizontal dashed line shows M^*_{UV}.

ORCID iDs

S. R. Kulkarni https://orcid.org/0000-0001-5390-8563
D. A. Perley https://orcid.org/0000-0001-8472-1996
A. A. Miller https://orcid.org/0000-0001-9515-478X

References

Abbott, B. P., Abbott, R., Abbott, T. D., et al. 2017a, PhRvL, 119, 161101
Abbott, B. P., Abbott, R., Abbott, T. D., et al. 2017b, ApJL, 848, L12
Arcavi, I., Gal-Yam, A., Kasliwal, M. M., et al. 2010, ApJ, 721, 777
Bellm, E., & Kulkarni, S. 2017, NatAs, 1, 0071
Blanton, M. R., & Moustakas, J. 2009, ARA&A, 47, 159
Cole, S., Norberg, P., Baugh, C. M., et al. 2001, MNRAS, 326, 255
Cook, D. O., Kasliwal, M. M., Van Sistine, A., et al. 2017, arXiv:1710.05016
Dekany, R., Smith, R. M., Belicki, J., et al. 2016, Proc. SPIE, 9908, 99085M
Droettboom, M., Caswell, T. A., Hunter, J., et al. 2018, Matplotlib/Matplotlib, V2.2.2, Zenodo, doi:10.5281/zenodo.1202077
Foley, R. J., Challis, P. J., Chornock, R., et al. 2013, ApJ, 767, 57
Foreman-Mackey, D. 2016, JOSS, 1, 24
Foreman-Mackey, D., Hogg, D. W., Lang, D., & Goodman, J. 2013, PASP, 125, 306
Galbany, L., Stanishev, V., Mourão, A. M., et al. 2016, A&A, 591, A48
Gehrels, N., Cannizzo, J. K., Kanner, J., et al. 2016, ApJ, 820, 136
Goliath, M., Amanullah, R., Astier, P., Goobar, A., & Pain, R. 2001, A&A, 380, 6
Graur, O., Bianco, F. B., Modjaz, M., et al. 2017, ApJ, 837, 121
Holoien, T. W.-S., Brown, J. S., Stanek, K. Z., et al. 2017a, MNRAS, 467, 1098
Holoien, T. W.-S., Stanek, K. Z., Kochanek, C. S., et al. 2017b, MNRAS, 464, 2672
Horiuchi, S., Beacom, J. F., Kochanek, C. S., et al. 2011, ApJ, 738, 154
Hunter, J. D. 2007, CSE, 9, 90
Jha, S., Riess, A. G., & Kirshner, R. P. 2007, ApJ, 659, 122
Jones, E., Oliphant, T., Peterson, P., et al. 2001, SciPy: Open Source Scientific Tools for Python, http://www.scipy.org/
Karachentsev, I. D., Makarov, D. I., & Kaisina, E. I. 2013, AJ, 145, 101
Kasliwal, M. M., Cenko, S. B., Singer, L. P., et al. 2016, ApJL, 824, L24
Li, W., Leaman, J., Chornock, R., et al. 2011, MNRAS, 412, 1441
Li, W. D., Filippenko, A. V., Treffers, R. R., et al. 2000, in AIP Conf. Ser. 522, Cosmic Explosions: Tenth Astrophysics Conf., ed. S. S. Holt & W. W. Zhang (Melville, NY: AIP), 103
McCray, R. 1993, ARA&A, 31, 175
McKinney, W. 2010, in Proc. 9th Python in Science Conf., ed. S. van der Walt & J. Millman, 51
Miller, A. A., Kasliwal, M. M., Cao, Y., et al. 2017, ApJ, 848, 59
Paturel, G., Petit, C., Prugniel, P., et al. 2003, A&A, 412, 45
Scannapieco, E., & Bildsten, L. 2005, ApJL, 629, L85
Scolnic, D. M., Jones, D. O., Rest, A., et al. 2017, arXiv:1710.00845
Smartt, S. J., Chambers, K. C., Smith, K. W., et al. 2016, MNRAS, 462, 4094
Sullivan, M., Conley, A., Howell, D. A., et al. 2010, MNRAS, 406, 782
Sullivan, M., Le Borgne, D., Pritchet, C. J., et al. 2006, ApJ, 648, 868
Taylor, M., Cinabro, D., Dilday, B., et al. 2014, ApJ, 792, 135
Tonry, J. L. 2011, PASP, 123, 58
Tully, R. B., Rizzi, L., Shaya, E. J., et al. 2009, AJ, 138, 323
Wainscoat, R., Chambers, K., Lilly, E., et al. 2016, in IAU Symp. 318, Asteroids: New Observations, New Models, ed. S. R Chesley et al. (Cambridge: Cambridge Univ. Press), 293
Wright, E. L. 2006, PASP, 118, 1711
Wyder, T. K., Treyer, M. A., Milliard, B., et al. 2005, ApJL, 619, L15
Yasuda, N., & Fukugita, M. 2010, AJ, 139, 39